SURFACE ANALYSIS OF SOLAR CELL COVER GLASSES AND OSR AFTER HIGH TEMPERATURE UV AND VUV EXPOSURE

Premysl Janik [(1)], Adrian Tighe [(1)], Christel Nömayr [(2)], Andreas Löhberg [(2)], Claus Zimmermann [(2)], Christopher Semprimoschnig [(1)]

[(1)] ESA-ESTEC, Keplerlaan 1, 2201 AZ Noordwijk, The Netherlands
premysl.janik@esa.int, adrian.tighe@esa.int, christopher.semprimoschnig@esa.int

[(2)] Airbus Defence and Space, 81663 Munich, Germany, christel.anke.noemayr@airbus.com, claus.zimmermann@airbus.com, andreas.loehberg@airbus.com

GLOSSARY

BC	BepiColombo
BOT	Beginning Of Test
DVT	Design Verification Test
EOT	End Of Test
ESH_{UV}	Equivalent Sun hours – UV range
ESH_{VUV}	Equivalent Sun hours – VUV range
FTIR	Fourier Transform Infrared Spectroscopy
HOPG	Highly Oriented Pyrolytic Graphite
MOC	Molecular Contamination
OSR	Optical Solar Reflector
QCM	Quartz Crystal Microbalance
TAMS	Total Absolute Measurement System
TOF-SIMS	Time-of-Flight Secondary Ion Mass Spectrometry
UV	Ultra Violet
VDA	Vacuum-deposited Aluminium
VUV	Vacuum Ultra Violet
XPS	X-ray photoelectron spectroscopy

ABSTRACT

The aim of our work was to investigate the degradation mechanisms involved, using detailed surface analysis techniques such as X-ray photoelectron spectroscopy (XPS) and Secondary-ion mass spectrometry (TOF-SIMS) depth profiling. Contamination witness samples exposed together with the main DVT test item hardware, and the surface chemistry of the samples was analysed in detail. Results from different exposures are presented, with varying UV dose and temperature, and possible degradation mechanisms discussed. The environmental conditions during the testing were also monitored in detail in order to determine possible correlation of results from surface analysis with the observed degradation. This included detailed characterisation of the in-situ contamination environment using quartz crystal microbalances (tQCM) and contamination witness plates. Considerable effort was also made to accurately measure the UV and VUV intensity on the samples and the methodology used is summarised.

1. INTRODUCTION

BepiColombo is the joint mission of the European Space Agency (ESA) and the Japanese Aerospace Exploration Agency (JAXA) to explore the planet mercury. The European contributions, namely the mercury transfer module (MTM) and the mercury planetary orbiter (MPO), are both powered by deployable solar arrays. Many materials and technologies are at their limit under the harsh high-intensity, high-temperature (HIHT) conditions of the mission. Synergistic effects like photo fixation and photo-enhanced contamination by ultra violet and vacuum ultra violet radiation (UV/VUV) on sunlit surfaces are considered to play an important role in the HIHT environment of the BepiColombo mission [1].

The design verification test (DVT) under UV/VUV conditions of sun-exposed materials and technologies on component level was part of the overall verification and qualification of the solar array design of the MTM and MPO presented in previous work [1]. Solar cell assemblies (SCAs), Optical solar reflectors (OSR) and other types of functional materials have been exposed to representative BepiColombo environment.

Present work consists of further exposure of OSR samples and detailed analysis of results from DVT test focusing on further degradation of OSR's performance.

2. EXPERIMENTAL

2.1. Initial design of the DVT test and motivation for its extension

The design of the BepiColombo Photovoltaic Assembly UV/VUV DVT test was prepared in collaboration with Airbus Defence and Space previously published in [1]. The initial set of 4 bonded OSR samples was exposed together with thermal control materials (coatings, VDAs), SCA's, and cable bundles in frame of 5 sequential UV/VUV exposure cycles reaching SCA's dose up to 30,000 ESH_{UV} [1]. During these initial 5 cycles the 4 bonded OSR samples were exposed to UV and VUV intensities up to 12 solar constants (SC_{UV}), and

temperatures ranging from 178 up to 197 ºC. Primary objective of DVT test was achieved and degradation of key properties on all sample types quantified [1]. Changes in the functional properties of the materials were observed, including increase in solar absorptance on the OSRs. Therefore in addition to the initial 5 another 3 UV/VUV cycles were required to reach another 30,000 UV ESH dose on bonded OSR samples exposed at temperature elevated to 240 ºC. For the exposure Cycles 6, 7 and 8 the SCAs and cable bundles were removed and "DVT-extended" test continued only for thermal control materials (VDAs and Keronite coatings) mostly focusing on two bonded OSR sample's (OSR-bonded) performance in terms of solar absorptance and normal thermal emittance. In addition to DVT test samples exposed during first 5 cycles, there had been several types of fresh witness samples added to the Cycle 6, 7 and 8 to enable better characterisation of contamination layers. Schematic of the sample plate is shown in the Figure 1. Note: The height of the exposed surface of witnesses and OSR-prist samples was lower than in case of OSR-bonded and VDA samples

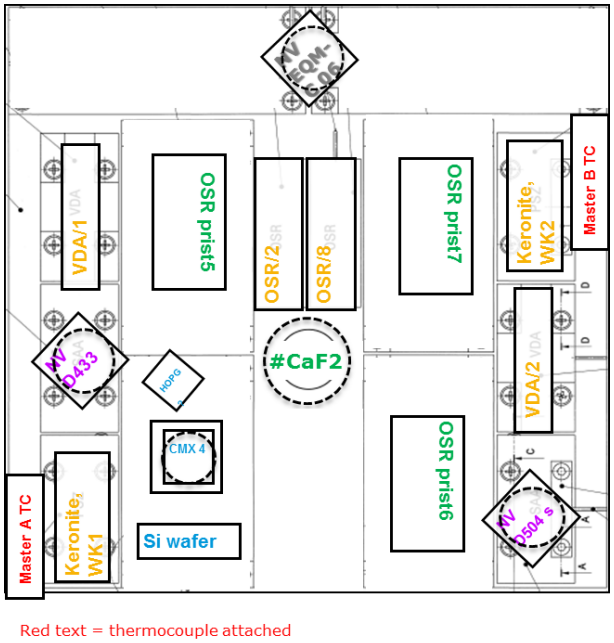

Figure 1: Schematic of sample distribution during BC DVT-extended exposures.

2.2. BC DVT-extended test samples and contamination witness samples

For the sequential contamination monitoring the Molecular contamination (MOC) monitoring CaF_2 witness window was used. In-situ MOC collectors were placed on two locations: cold shroud and centre of the sample plate. Both MOC windows were analysed by ex-situ MOC FTIR analysis and UV-VIS-NIR transmission. Semi quantitative MOC FTIR analysis was used to distinguish between 4 functional groups contributing to collected contamination: A – Hydrocarbons, B – Esters, C –Methyl silicones, C*- Silica-like, D-Methyl-phenyl silicones.

There was also tQCM micro balance attached to the cold shroud and kept at -40 ºC to enable in-situ monitoring of contamination background during all 8 DVT UV/VUV exposure cycles. In addition to MOC and QCM which were used in all 8 cycles, another types of witnesses, XPS witnesses (HOPG, borosilicate cover glass CMX and Si-wafer) and 3 pristine OSRs were introduced to the DVT-extended test (exposure Cycles 6,7 and 8). Fresh pristine OSRs (OSR-prist) samples replaced positions of SCAs on the original DVT sample plate.

2.3. The UV/VUV exposure facility and experimental conditions

As described previously in [1] the DVT UV/VUV exposure cycles were conducted in the CROSS1 vacuum facility at ESA/ESTEC. The facility offers exposure to UV (up to 12 SC) as well as VUV (up to 9SC). The base plate of the facility can be heated and cooled to control the sample temperature. The UV intensity varied between 7 and 12 solar constants (SC) across the sample plate. The stability of VUV intensity depends on contamination background around the VUV lamp is inside the vacuum chamber. Because of this fact, frequent intermediate VUV lamp cleaning steps were undertaken. The measured VUV intensity itself was lower compared to the UV intensity. This was predominantly related to the aspect angle of 45° of the VUV illumination. The measured values ranged from <1 to 16 SC_{VUV}.

Temperature of the sample plate was initially controlled to achieve average SCA's temperature (Cycles 1-4 at 200ºC with durations 200, 400, 800, 1000, Cycle 5 at 215ºC for 600 hours, which corresponded to and later on controlled based on temperature of remaining two OSR-bonded samples (Cycle 6-8 at 240ºC for 500, 1300 and 650 hours). The temperature OSR-prist samples as well as contamination witness samples were not controlled. OSR-prist sample temperature was estimated by infrared camera to be at 185 ºC. Cold shroud temperature was controlled at -175 ºC. Pressure in the facility was controlled and kept bellow 5×10^{-6}mBar.

2.4. Surface characterisation techniques

The following techniques were used for post-test ex-situ characterisation of exposed samples:

Visual inspection:	all samples
Solar absorptance (α):	OSR-bonded and OSR-prist
Thermal emittance (ε):	OSR-bonded and OSR-prist
XPS:	HOPG, CMX, Si-wafer and OSR-prist

TOF-SIMS: HOPG, CMX, OSR-prist, OSR-bonded, Si-wafer

The TOF-SIMS analyses were carried out externally (Aystorm Scientific) using an ION-TOF V instrument. The depth profiling was carried out using an Ar cluster source (5keV, 1.1nA , 1400 atoms/ cluster) on areas of 350 × 350 µm for sputtering and a Bismuth source for data acquisition under static SIMS conditions (Figure 2). The erosion rate of the organic constituents was calibrated using reference organics with known thickness. Thickness was determined with accuracy of 0.5 nm.

3. RESULTS

3.1. Cumulative UV/VUV exposure dosage obtained on the samples

Because of non-uniformity in UV/VUV intensity across the sample plate and during each test cycle a significant effort was dedicated to BOT and EOT radiation intensity evaluation at all sample locations.

Table 1: Cumulative ESH_{UV} dosage for individual samples

UV position	Sample	Cy5	Cy6	Cy7	Cy8
5	XPS witnesses	-	5155	18522	25382
6	OSRprist5	-	5301	19152	26210
8	OSR/1	33659	-	-	-
9	**OSR/2**	**34563**	**39972**	**54239**	**61472**
10	**CaF2 witnesses**	**35621**	**41183**	**55750**	**63166**
11	OSR/3	33564	-	-	-
12	**OSR/8**	**34545**	**39939**	**53997**	**61148**
13	OSRprist6	-	4972	17595	24151
14	OSRprist7	-	5022	18013	24616

Table 2: Cumulative ESH_{VUV} dosage for individual samples

VUV position	Sample	Cy5	Cy6	Cy7	Cy8
5	XPS witnesses	-	4129	13200	18522
6	OSRprist5	-	4661	15318	22077
8	OSR/1	26014	-	-	-
9	**OSR/2**	**32117**	**38675**	**53917**	**63030**
10	**CaF2 witnesses**	**37716**	**43306**	**57768**	**65741**
11	OSR/3	24083	-	-	-
12	**OSR/8**	**25630**	**31175**	**45366**	**53016**
13	OSRprist6	-	3936	14068	19590
14	OSRprist7	-	4900	16914	24141

Note: OSR-bonded samples OSR/1 and OSR/3 were removed from DVT-extended sample set and analysed as Cycle6 BOT reference point.

3.2. Visual characterisation

Unlike the thermal control coating showing darkening already after first thousands of ESH_{UV} (reported in previous work [1]) there were no visible changes observed on OSR-bonded surfaces after the dose up to 63,000 ESH_{UV}. OSR-bonded samples remained well attached to their individual support plates without any signs of cracks. OSR-prist samples were located in the areas where significant darkening of the sample plate occurred after exposure cycles 6, 7 and 8. The appearance of OSR exposure areas before Cycle 6 and after Cycle 8 are shown in the Figure 2.

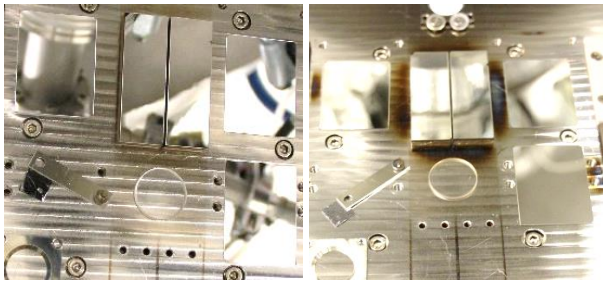

Figure 2: Appearance of BC DVT sample plate before exposure Cycle 6 (left) and after last exposure Cycle 8 (right)

3.3. Thermo-optical properties

Evolution of solar absorptance of UV/VUV exposed OSRs as a function of ESH_{UV} is plotted in the Figure 3. The solar absorptance of OSR-prist samples (5,6 & 7) added to the test from Cycle 6 increased much faster than already exposed OSR-bonded samples with two times more ESH_{UV} dosage. This could be associated with the difference in temperature exposure or location on the sample plate when compared to situation for OSR-bonded samples. Similar trend was recorded also for ESH_{VUV} dosage.

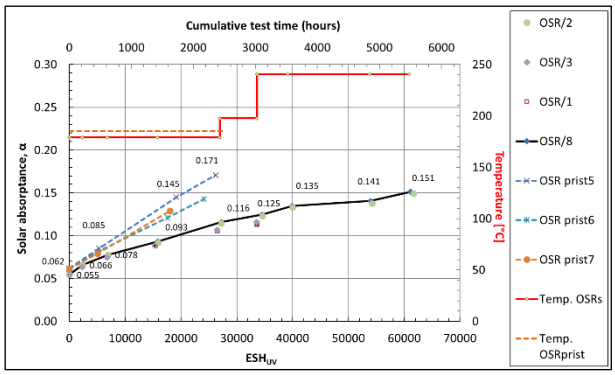

Figure 3: Solar absorptance of various OSR samples as function of ESH_{UV}

A detailed study of OSR-prist samples proved that the darkening observed on the sample plate was also identified in solar absorptance profile of OSR, increasing α values from 0.18 (in the centre of OSR) up to 0.22 (towards the edges closer to major the contamination sources). The visualisation of the profile is displayed in

the Figure 4. The darkening effects were more obvious on the areas close to the samples than on exposed samples themselves. These effects are probably associated with higher outgassing rates from OSR-bonded and VDA samples during Cycles 6 – 8 where the temperature was 240-250 ºC, much higher than during Cycles 1-5 (178-197 ºC).

The initial value of normal thermal emittance, ε = 0.82, did not change significantly on any of exposed OSRs.

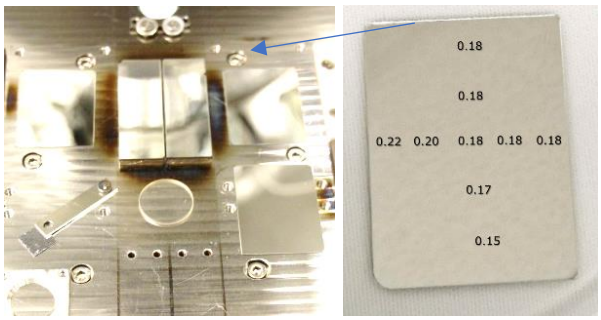

Figure 4: Solar absorptance profile on OSR-prist as a function of position

3.4. Contamination monitoring

The cumulative plots of contamination during all 8 UV/VUV exposure cycles is shown in the Figure 5.

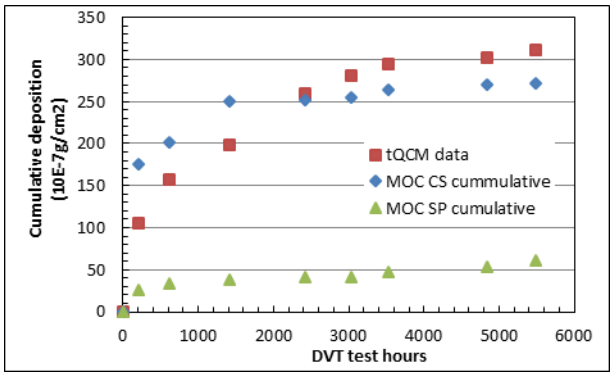

Figure 5: Evolution of cumulative deposition of contamination based on analysis of MOC FTIR windows on two locations and tQCM frequency

The cumulative MOC collected on the cold shroud (MOC CS cumulative) matches well with delta frequency build-up observed on tQCM reaching up to 310×10^{-7}g/cm^2. The MOC CaF_2 witness window located at the centre of the sample plate (at the temperatures 200, 215 and up to 250 ºC respectively and high UV/VUV dosage, MOC SP cumulative in the Figure 5) collected 4 times less contamination than MOC witness on the cold shroud exposed at -175 ºC to limited UV and no VUV radiation. Nevertheless both showed decrease in deposition rates in time which is related to depletion of sources during the test. Semi-quantitative FTIR analysis of MOC CaF_2 witness identified C*-type (Silica-like) contamination reaching up to 16.3 $\times10^{-7}$g/cm^2 on the sample plate location after Cycle 6, 7 and 8 (dose>25000ESH$_{UV}$). Note that during Cycle 6, 7 and 8 the cumulative MOC contamination levels 11.7×10^{-7}g/cm^2 (C-methyl silicone and C* silica-like) on the cold shroud area were lower than a total contamination collected during the same test cycles on the sample plate. Assuming that silicone-containing contaminants have density approx. 1.5g/cm^3, then the cumulative contamination thickness on CaF_2 witness would reach up to 10.3 nm at the end of Cycle 8 (after dose 27,500 ESH$_{UV}$).

3.5. XPS analysis of exposed surfaces

The most noticeable evolution in surface layer composition was identified at the surfaces of CMX cover glasses (Figure 6) and HOPG (Figure 7).

The coverage of HOPG (Figure 7) with methyl-silicone and silica-like contaminants, which were dominating DVT Cycles 6, 7 and 8, resulted in increase of relative concentration of silicon and oxygen on the surface (-Si$_x$O$_y$) and relative attenuation of carbon from the graphitic substrate. Similar behaviour shows also the relative concentration of carbon on CMX's borosilicate cover glass substrate (Figure 6) The signal from antireflective coating (AR) coating (Mg, F) is attenuating, being covered by organic contaminants (C).

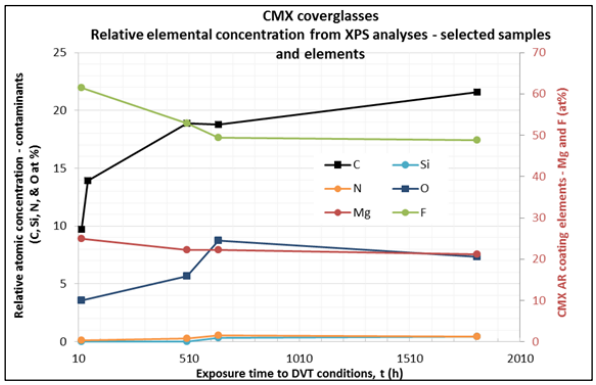

Figure 6: XPS- Elemental composition of contamination layers collected on CMX witness during DVT-extended test

Possible source of the remaining contaminants were probably phenyl methyl-silicone based adhesives used in OSR-bonded samples and VDA samples. XPS characterisation technique proved to be very sensitive, considering relatively low contamination background in exposure Cycles 6, 7 and 8, which was 10-20 times lower than during first cycles (Detailed MOC FTIR analysis proved that the MOC witnesses did not collect hydrocarbons nor esters during the last test cycles). Based on Mg1s spectral signal attenuation in CMX cover

glass spectrum, the initial contamination thicknesses of unexposed CMX were estimated to be 2-3 nm. This thickness proved to be unchanged after 24h cleanliness assessment in empty chamber using same experimental conditions (UV/VUV, temperatures). This is in line with FTIR MOC values, which were below detection limits for every cleanliness assessment between each two consecutive exposure cycles. After exposure during Cycle 6 and 7 (CMX's total dose 18522 ESH_{UV}) contamination thickness was estimated to be 4-4.5 nm using the same XPS signal attenuation methodology.

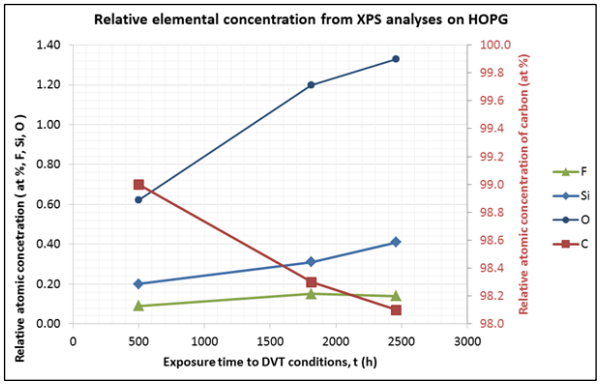

Figure 7: XPS- Elemental composition of contamination layers collected on HOPG witness during DVT-extended test (Cycles 6, 7 and 8)

3.6. TOF-SIMS depth profiling

In addition to MOC-FTIR and XPS-attenuation also TOF-SIMS depth profiling method was used to determine contamination thicknesses. Figure 8 shows comparison of estimated thicknesses on different substrates as a function of ESH_{UV} dosage.

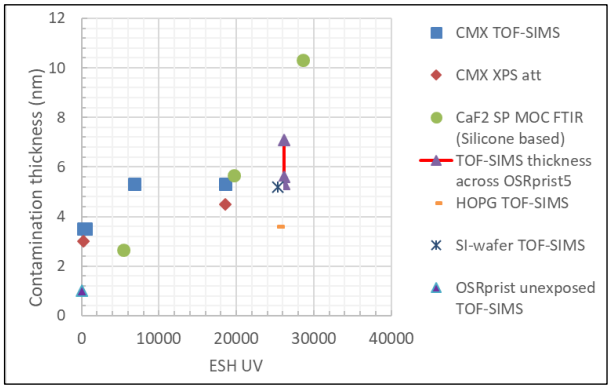

Figure 8: Comparison of values from various samples and thickness determination techniques as a function of ESH_{UV} dose

As it is visible from the Figure 8, the range of obtained thicknesses using various techniques is consistent for all three methodologies. Thickness of contamination layers determined by TOF-SIMS on various samples ranges between 3.8 to (HOPG) and 7.1 nm (OSR-prist5, edge closer to contamination source). Figure 9 visualises a similarity in dependence of contamination thickness and solar absorptance at centre of OSR-prist sample on ESH_{UV} dose.

A detailed TOF-SIMS signal analysis from OSR-prist5, the thickest contamination layer observed in DVT test, is shown in the Figure 10.

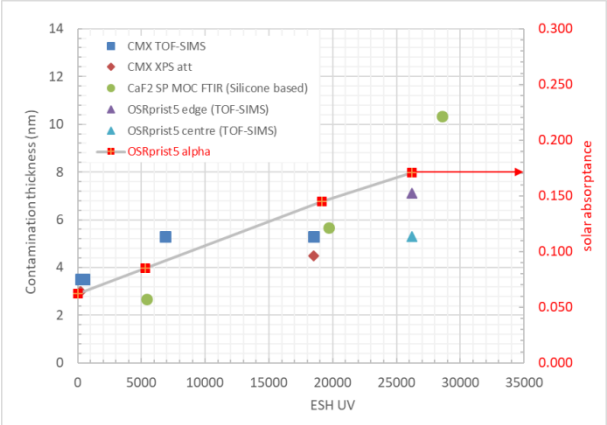

Figure 9: Comparison of contamination thickness values from various samples and thickness determination techniques (left axes) correlating with growth in OSR-prist solar absorptance (right axes) as a function of ESH_{UV} dose.

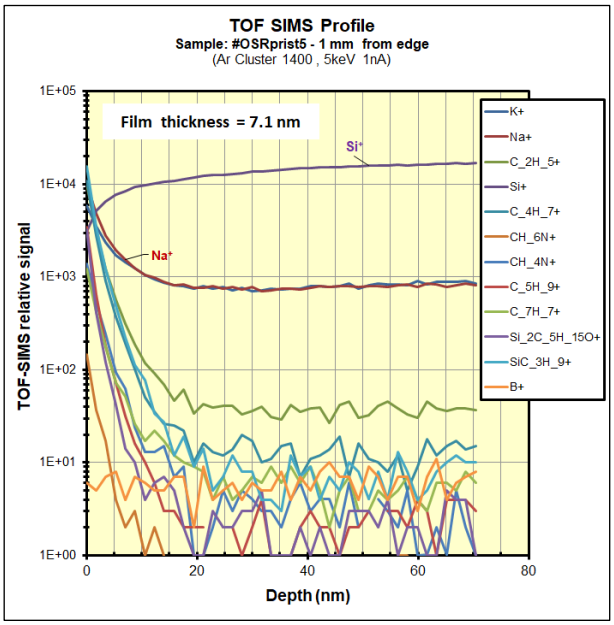

Figure 10: TOF-SIMS depth profiles of various contamination components residing on OSR-prist5 sample after UV/VUV exposure (total dose >26000 ESH_{UV})

The Figure 11 represents the comparison of contamination thicknesses determined by TOF-SIMS for of all tested OSRs and two different trends of increase in solar absorptance.

Note that even with minimal contamination thickness, observed on OSR-bonded samples, the solar absorptance was still increasing.

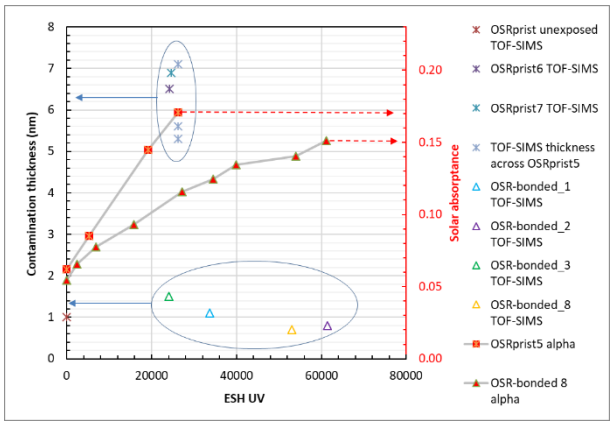

Figure 11: Two different clusters of contamination thicknesses representing two different sensitivities of OSR's contamination to ESH_{UV} dose

4. DISCUSSION

Two different clusters of contamination thicknesses (Figure 11) clearly indicated two families of results: one from the OSR-bonded samples and second from the OSR-prist samples. OSR-prist (free, lower laid OSRs) had their contamination layers significantly thicker than those observed on OSR-bonded samples. For the OSR-bonded samples the evolution in solar absorptance did not follow the evolution in contamination thickness as it was in OSR-prist samples cases, but their solar absorptance grew instead, while the contamination thickness decreased below 1 nm with further ESH_{UV} dose. This suggests that there are independent mechanisms of contamination deposition on the one hand and photochemical reactions of the deposited contamination on the other hand. The change in solar absorptance due to contamination under UV/VUV is not only depending on the applied dose but also depends on the deposition rates and the photochemical ageing of the contamination layers which are parallel mechanisms, depending on even more complex parameters, e.g. chemical nature of contamination and so on.

Other approaches, using an injection of pre-defined contamination type and the representative temperature steps on thermal control substrates (e.g. TML approach, [2]), may simulate the real situation on the flight hardware. On the other hand, the used UV/VUV DVT test methodology proved that even with very conservative, contamination-rich environment, the OSR samples did not collect very thick contamination layers but proved to be sensitive to UV/VUV darkening. Using contamination thickness determination in combination with DVT methodology, contamination-accelerated test can further tuned for future needs in contamination impact investigations.

Combining the findings from evolution in solar absorptance from different locations/temperature of exposed OSR samples (Figure 3) and evolution in cumulative contamination (Figure 5) the most critical parameters in the solar absorptance evolution of UV/VUV exposed OSRs probably are:

- contamination thickness
- total UV/VUV dose (ESH)

but possibly also:

- exposure temperature
- location of the exposed surfaces with respect to contamination sources
- composition of contamination and
- stability of bonded OSR's interface/silver layer

When it comes on assessment of the impact on solar absorptance and risk of OSRs darkening, the nature of the contaminants (silicones vs. hydrocarbons) might be more important than total contamination thickness. TOF-SIMS thickness data suggest that the carbon-rich contamination would have much higher darkening potential than silicone rich contamination.

The stability and long-term reflectance of the bonded OSRs at elevated temperatures under UV/VUV radiation should be further studied in order to discriminate other possible effects increasing the solar absorptance such as chemical interaction between adhesive and silver layers or thermally-induced stresses, physically deteriorating functional coating in OSR.

CONCLUSIONS

In frame of BC DVT UV/VUV test support a valuable solar absorptance data over 60,000 $ESH_{UV/VUV}$ were obtained from bonded OSR samples.
Several experimental techniques were used to study the evolution of contamination thickness and its impact on thermo-optical properties over a duration up to 5400 test hours. Three methodologies for contamination thickness determination were demonstrated (MOC FTIR, XPS attenuation and TOF-SIMS), using various collection substrates including CMX cover glasses and other materials, enabling to follow specific contamination constituents.
Two sets of OSR samples with different histories showed different behaviour in terms of response of solar absorptance on total contamination thickness and on $ESH_{UV/VUV}$ dose. Further development in the test methodology and modelling is therefore needed, to better describe long-term performance of thermal control materials under UV/VUV exposure conditions.

ACKNOLEDGEMENTS

Authors would like to thank to all their colleagues from ESA's and ADS's M&P teams, which have contributed to this work. Special thanks to Y. Butenko, R. Martins,

N. Dias, B. Bras, G. Milassin and G. van Papendrecht (ESA/TEC-QEE section) for their contribution to the DVT test and to H. Kheyrandish (Aystorm Scientific) for the TOF-SIMS depth profiling and XPS-based thickness analyses.

REFERENCES

1. Nömayr, C. et al. Degradation of Solar Array Components in a Combined UV/VUV High Temperature Test Environment. *E3S Web of Conferences.* 16. 04007, 2017
DOI: 10.1051/e3sconf/20171604007

2. Y. V. Butenko et al., Effect Of Space Environment On NV14 Ceramic White Coating Of High Gain Antenna Of BepiColombo Spacecraft: Long Duration Test (*Proceedings of the 14th ISMSE/12th ICPMSE*, Biarritz, France, 1-5th October 2018)